Desalination and Water Treatment 8 (2009) 201–210
www.deswater.com
1944-3994/1944-3986

Sorption of malachite green by eucalyptus bark as a non-conventional low-cost biosorbent

Sihem Boutemedjet[a,b], Oualid Hamdaoui[a]*

[a]*Laboratory of Environmental Engineering, Department of Process Engineering, Faculty of Engineering, University of Annaba, P.O. Box 12, 23000 Annaba, Algeria*
Tel. +213 771 59 85 09; email: oualid.hamdaoui@univ-annaba.org, ohamdaoui@yahoo.fr
[b]*Department of Chemistry, Faculty of Sciences, University of Annaba, P.O. Box 12, 23000 Annaba, Algeria*

Received 8 March 2009; accepted 18 June 2009

ABSTRACT

In this work, eucalyptus bark, a forest waste, was evaluated for its ability to remove malachite green (MG) from aqueous solutions. Sorption kinetic experiments were studied in a batch mode operation at various initial dye concentrations, sorbent dosages, and temperatures. The equilibrium sorption data of MG by eucalyptus bark were analyzed by Langmuir and Freundlich isotherm models. The results indicate that both the Langmuir and Freundlich equations provide good correlation of the experimental data, but the Langmuir expression fits the equilibrium data better. The maximum sorption capacity of eucalyptus bark was found to be 59.88 mg g^{-1} at 20 °C. Pseudo-first-order, pseudo-second-order, and intraparticle diffusion models were used to analyze the kinetic data obtained at different concentrations. Among the kinetic models studied, the pseudo-second-order was the best applicable model to describe the sorption of MG by eucalyptus bark. The overall rate of dye uptake was found to be controlled by external mass transfer at the beginning of sorption, while intraparticle diffusion controlled the overall rate of sorption at a later stage. The results indicate the potential of eucalyptus bark as biosorbent for the removal of basic dye from aqueous solution.

Keywords: Malachite green; Eucalyptus bark; Batch mode; Sorption kinetics; Sorption isotherm

1. Introduction

Discharge of colored wastewater from various industries is currently a major problem for environmental management in many countries. Color is a visible pollutant and the presence of even very minute amount of coloring substance makes it undesirable due to its appearance. Basic dyes have high brilliance and intensity of colors and are highly visible even in a very low concentration [1]. Malachite green (MG), a basic dye, is most widely used for coloring purpose, amongst all other dyes of its category [2]. MG was found to be toxic to human cells and might cause liver tumor formation. The use of this dye has been banned in several countries and not approved by US Food and Drug Administration. However, due to its ease and low cost to manufacture, it is still used in certain countries with less restrictive laws for non-aquaculture purposes. Hence, the dye removal is of great importance.

Several techniques have been used for the removal of dyes from industrial effluents. In comparison with other methods, adsorption has been found to be superior in terms of simplicity of design, initial cost, ease of operation, and insensitivity to toxic substances.

*Corresponding author

Although activated carbon is the most effective adsorbent for adsorption of dye, it is quite expensive and hence there is an increasing need for equally effective but cheaper adsorbent. Extensive research has been undertaken recently to develop alternative and economic adsorbents. A number of non-conventional sorbents has been reported in the literature for their capacity to remove MG from aqueous solutions, such as de-oiled soya [3], agro-industry waste, *Prosopis cineraria* [4], bagasse fly ash [5], hen feathers [6], iron humate [7], modified rice straw [8], orange peel [9], rice husk [10], etc.

In this investigation, we attempt to use eucalyptus bark as an alternative low-cost sorbent in the removal of MG from aqueous solutions. To our knowledge, the sorption of dyes in the solutions using eucalyptus bark was little studied. Morais et al. [11,12] reported the adsorption of reactive dyes from aqueous solutions on eucalyptus bark. Saliba et al. [13] have studied the removal of reactive dyes (Acid Blue 25, Eriochrome Blue Black B, and Calmagite) by formaldehyde pretreated eucalyptus bark powder. The validity of the results for basic dyes needs further investigation.

The objective of this work was to investigate the potential of eucalyptus bark, a forest solid waste, as a novel sorbent in the removal of the basic dye, MG, from aqueous solutions. The effects of various operating parameters such as initial dye concentration, sorbent dosage, and temperature on dye removal were investigated. The sorption mechanism was determined.

2. Materials and methods

2.1. Sorbate

The cationic basic dye (C.I. 42000; Basic Green 4), MG oxalate salt, (molecular formula $C_{52}H_{56}N_4O_{12}$, FW 929), was obtained from Merck and used without further purification. Fig. 1 displays the structure of this dye.

2.2. Sorbent

Eucalyptus bark used in the present work was collected in autumn 2005 from adult trees from the University Scientific Campus of Sidi-Amar, Annaba, Algeria. The collected bark was washed with permuted water several times to remove dirt particles and water soluble materials. The washing process was continued till the wash water contained no color. The washed materials were then completely dried in an oven at 80 °C for 24 h. The dried barks were then cut into small pieces, crushed, and sieved to eliminate fine particles (<0.5 mm). The obtained material was washed repeatedly

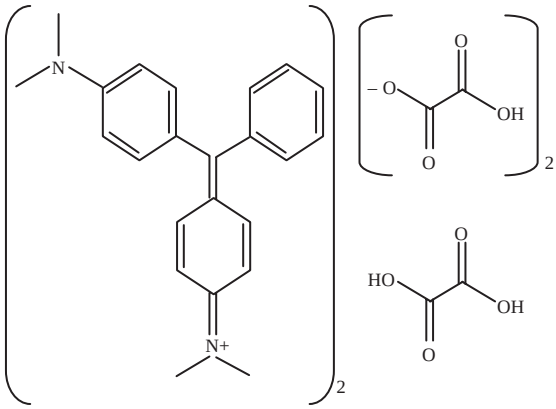

Fig. 1. Chemical structure of MG (oxalate salt).

with distilled water (conductivity 0.5 μS cm^{-1} and pH 6) until the wash water contained no color and its UV/Vis absorbance (200–700 nm) was equal to zero and electric conductivity and pH remain constant. Finally, the obtained material was then dried in an air circulating oven at 80 °C for 2 days and stored in a desiccator until use.

The macroscopic structure of eucalyptus bark particles is shown in Fig. 2. The surface structure of eucalyptus bark was analyzed by scanning electronic microscopy (SEM) at two different magnifications. The textural structure examination of eucalyptus bark particles can be observed from the SEM photographs at 1000× and 5000× magnifications (Fig. 3a and b). These photographs reveal that eucalyptus bark exhibits a caves-like, uneven, and rough surface morphology.

2.3. Effect of initial dye concentration

A mass of 0.4 g of eucalyptus bark was contacted with 200 mL MG solutions of dye concentrations

Fig. 2. Macroscopic structure of eucalyptus bark particle.

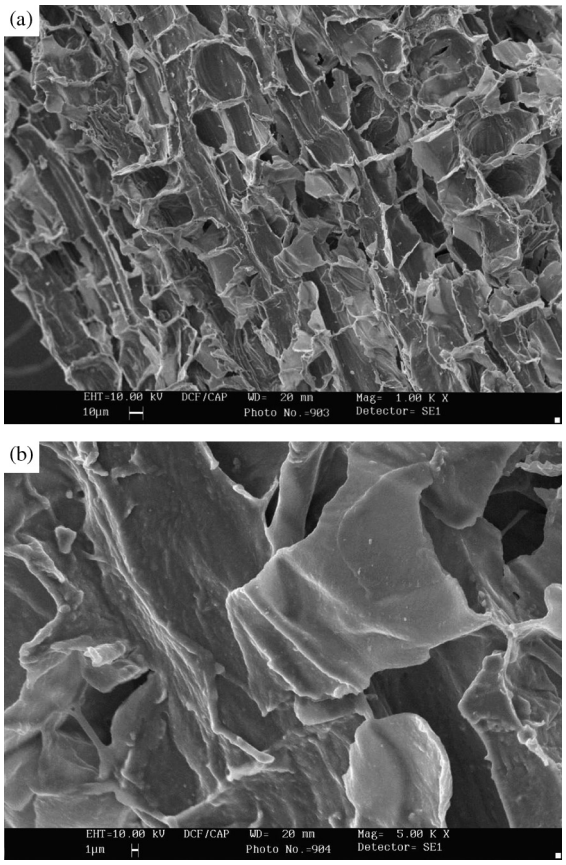

Fig. 3. SEM micrograph of eucalyptus bark particle: (a) magnification 1000× (b) magnification 5000×.

10–50 mg L^{-1} (pH 5) using water-bath maintained at 20 °C. The agitation speed was kept constant at 400 rpm. At predetermined intervals of time, samples were analyzed for the final concentration of MG by a UV/Vis spectrophotometer (Hewlett Packard 8453) at a wavelength of 618 nm, maximum absorbance.

The dye removal percentage can be calculated as follows:

$$\text{Removal percentage} = \frac{C_0 - C_e}{C_0} \times 100 \quad (1)$$

where C_0 and C_e (mg L^{-1}) are the initial and equilibrium liquid-phase concentrations of dye, respectively.

2.4. Effect of sorbent dosage

Samples of eucalyptus bark (0.2, 0.4, 0.6, 0.8, and 1.0 g) were added to 200 mL dye solution. The initial dye concentration was 50 mg L^{-1} (pH 5) at constant temperature (20 °C) and stirring (400 rpm).

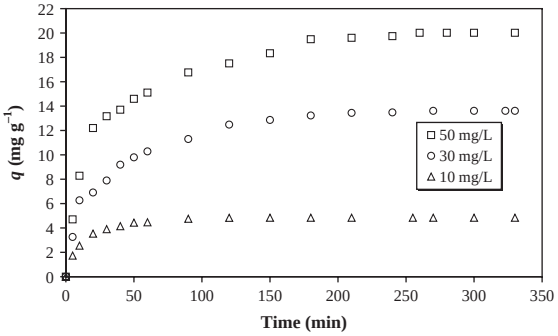

Fig. 4. Effect of contact time and initial dye concentration on MG sorption by eucalyptus bark (sorbent dose = 0.4 g/200 mL, $T = 20$ °C, pH 5).

2.5. Effect of temperature

The effect of temperature (at 20, 35, and 50 °C) on the sorption of MG by eucalyptus bark sorbent was studied at 0.4 g sorbent and initial MG concentration of 50 mg L^{-1} (pH 5) for 8 h contact time.

2.6. Equilibrium studies

Batch sorption isotherm was carried out by adding a fixed amount of sorbent (0.4 g) into 200 mL of different initial concentrations (25–300 mg L^{-1}) of dye solution at pH 5. The suspensions were stirred at 400 rpm and 20 °C for 8 h until equilibrium was reached. Aqueous samples were taken from the solutions and the concentrations were determined.

3. Results and discussion

3.1. Effect of contact time and initial concentration

Fig. 4 shows the effect of contact time and initial MG concentration on the removal of dye by eucalyptus bark. The sorption efficiency of MG increased gradually with increasing contact times and reached a plateau afterwards. At this point, the amount of dye being sorbed onto the sorbent was in a state of dynamic equilibrium with the amount of dye desorbed from the sorbent. The contact time needed for MG solutions with initial concentrations of 30 and 50 mg L^{-1} to reach equilibrium was 270 min. For MG solution with an initial concentration of 10 mg L^{-1}, equilibrium time of 150 min was required. This is due to fact that sorption sites took up the available dye more quickly at low concentration, but dye needed to diffuse to the inner sites of the sorbent for high concentration. Additionally, the curves of contact time are single, smooth, and continuous leading to equilibrium. These curves

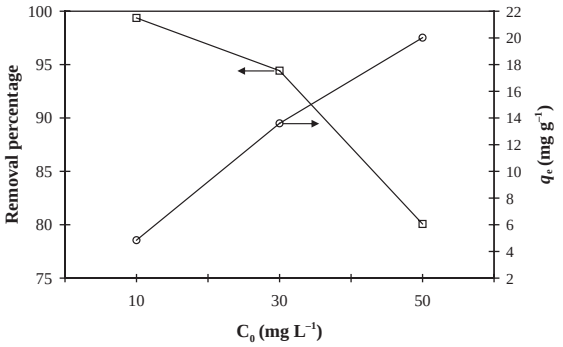

Fig. 5. Evolution of dye removal percentage and sorbed amount at equilibrium versus initial concentration (sorbent dose = 0.4 g/200 mL, T = 20 °C, pH 5).

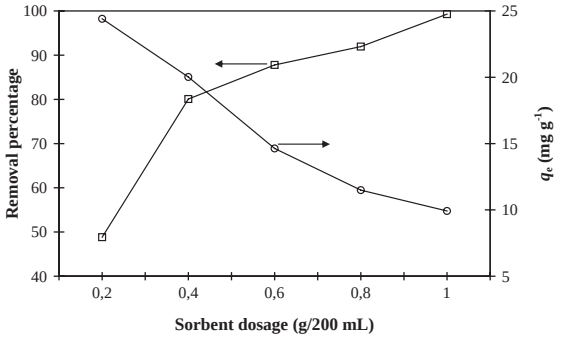

Fig. 6. Evolution of dye removal percentage and sorbed amount at equilibrium versus sorbent dosage (C_0 = 50 mg L^{-1}, T = 20 °C, pH 5).

indicate the possible monolayer coverage of dye on the surface of eucalyptus bark. From Figs. 4 and 5, it was observed that the dye removal varied with varying initial MG concentration. It was noticed that an increase in initial dye concentration leads to an increase in the sorption capacity of MG by eucalyptus bark. Equilibrium uptake increased with the increase of initial dye concentration at the range of experimental concentration (Fig. 5). This is a result of the increase in the driving force the concentration gradient, as an increase in the initial dye concentrations. When initial MG concentration was increased from 10 to 50 mg L^{-1}, the equilibrium sorption capacity increased from 4.84 to 20.02 mg g^{-1}. The initial rate of sorption was greater for higher initial MG concentration (Fig. 4), because the resistance to the dye uptake decreased as the mass transfer driving force increased. The rapid sorption observed during the first 20 min is probably due to the abundant availability of active sites on the eucalyptus bark particle surface, and with the gradual occupancy of these sites, the sorption becomes less efficient. It is also noticed in Fig. 5 that an increase in the initial MG concentration leads to a decrease in the percentage of MG removal. As the initial MG concentration increases from 10 to 50 mg L^{-1} the equilibrium removal of MG decreases from 99.4% to 80.1%. This effect can be explained as follows: at low dye/sorbent ratios, there are number of sorption sites in eucalyptus bark structure. As the dye/sorbent ratio increases, sorption sites are saturated, resulting in decreases in the sorption efficiency.

The sorption process could be divided into three regimes (Fig. 4): the sorption is increased instantly at initial stages (due to rapid attachment of dye to the surface of the sorbent), and then keeps increasing gradually until the equilibrium is reached and remains constant. The second regime was slower possibly because adsorption took place in the sorbent network.

3.2. Effect of sorbent dosage

The effect of sorbent dosages on the amount of MG sorbed at equilibrium and the removal percentage of dye is shown in Fig. 6. An increase in the eucalyptus bark dose from 0.2 to 1 g/200 mL increases the percentage of dye removal from aqueous solution from 48.8% to 99.2%. This may be attributed to increased sorbent surface area and availability of more sorption sites resulting from the increased dose of the sorbent. On the other hand, the amount of MG sorbed at equilibrium decreases from 24.41 to 9.92 mg g^{-1} with an increase in sorbent dosage between 0.2 and 1 g/200 mL. The increase in sorbent dose at constant dye concentration and volume will lead to unsaturation of sorption sites through the sorption process. At higher eucalyptus bark to dye concentration ratios, there is a superficial sorption onto the sorbent surface that produces a lower dye concentration in the solution than when the sorbent to dye concentration ratio is lower. This is because a fixed mass of eucalyptus bark can only sorb a certain amount of dye. Therefore, the higher the sorbent dosage is, the larger the volume of effluent that a fixed mass of eucalyptus bark can purify is. The decrease in the amount of MG sorbed with increasing sorbent dose is due to the split in the flux or the concentration gradient between MG concentrations in the solution and on the sorbent surface. Additionally, this decrease may be attributed to overlapping or aggregation of sorption sites resulting in decrease in total sorbent surface area available to dye and an increase in diffusion path length [14].

3.3. Effect of temperature

The sorption studies were carried out at three different temperatures 20, 35, and 50 °C, and the results of these experiments are shown in Fig. 7. Both the sorption capacity and the removal percentage of MG

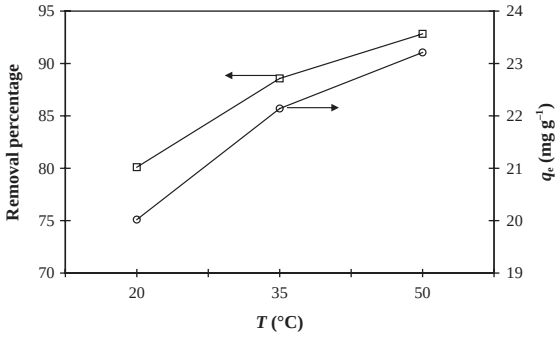

Fig. 7. Evolution of dye removal percentage and sorbed amount at equilibrium versus temperature (sorbent dosage = 0.4 g/200 mL, C_0 = 50 mg L^{-1}, pH 5).

increase with the increasing temperature, indicating that the sorption is an endothermic process. This may be a result of increase in the mobility of the dye with increasing temperature. Furthermore, the enhancement in the sorption capacity might be due to the enhancement of sorptive interaction between the active sites of sorbent and sorbate ions, creation of some new sorption sites or the increased rate of intraparticle diffusion of MG molecules into the pores of the sorbent at higher temperatures [15–17]. The removal percentage of MG increased from 80.1% to 92.8% with the rise of temperature from 20 to 50 °C, respectively. The amount of dye sorbed at equilibrium is determined as 20.02, 22.14, and 23.21 mg g^{-1} at 20, 35, and 50 °C, respectively.

3.4. Isotherm analysis

The distribution of MG between the sorbent and the aqueous solution at equilibrium has been expressed using the two widely used models the Langmuir and the Freundlich isotherms.

3.4.1. Langmuir model

The Langmuir model assumes uniform energies of adsorption onto the surface and no transmigration of adsorbate in the plane of the surface. The Langmuir equation may be written as

$$q_e = \frac{q_m b C_e}{1 + bC_e} \quad (2)$$

where q_e is the amount of solute sorbed per unit weight of sorbent (mg g^{-1}), C_e is the equilibrium concentration of the solute in the bulk solution (mg L^{-1}), q_m is the monolayer sorption capacity (mg g^{-1}), and b (L mg^{-1}) is the constant related to the free energy of sorption.

Eq. (2) can be linearized as follows:

$$\frac{C_e}{q_e} = \frac{1}{q_m} C_e + \frac{1}{q_m b} \quad (3)$$

The sorption data were analyzed according to the linear form of the Langmuir isotherm. The plot of C_e/q_e versus C_e gives a straight line of slope $1/q_m$ and intercept $1/bq_m$ (figure not shown). The isotherm was found to be linear over the entire concentration range studied with a good linear regression coefficient (R^2 = 0.993), showing that data correctly fit the Langmuir model. The Langmuir parameters are tabulated in Table 1. The monolayer saturation capacity was found to be 59.88 mg g^{-1}. The fact that Langmuir isotherm fits the experimental data very well confirms the monolayer coverage of dye onto sorbent particles and also the homogenous distribution of active sites on the material, since the Langmuir equation assumes that the surface is homogenous.

The favorable nature of sorption can be expressed in terms of dimensionless separation factor of equilibrium parameter, which is defined by [18]:

$$R_L = \frac{1}{1 + bC_0} \quad (4)$$

where b is the Langmuir constant and C_0 is the initial concentration of the sorbate in solution.

The values of R_L indicates the type of isotherm to be irreversible (R_L = 0), favorable (0 < R_L < 1), linear (R_L = 1) or unfavorable (R_L > 1). The calculated R_L values versus initial MG concentration were represented in Fig. 8. From this figure, it was observed that sorption was found to be more favorable at higher concentrations. Also the value of R_L in the range of 0–1 at

Table 1
Parameters of the Langmuir and Freundlich isotherms for the sorption of MG by eucalyptus bark

Langmuir			Freundlich		
q_m (mg g^{-1})	b (L mg^{-1}) × 10^3	R^2	K_F (mg$^{1-\frac{1}{n}}$ L$^{\frac{1}{n}}$ g^{-1})	n	R^2
59.88	72.93	0.993	8.41	2.55	0.986

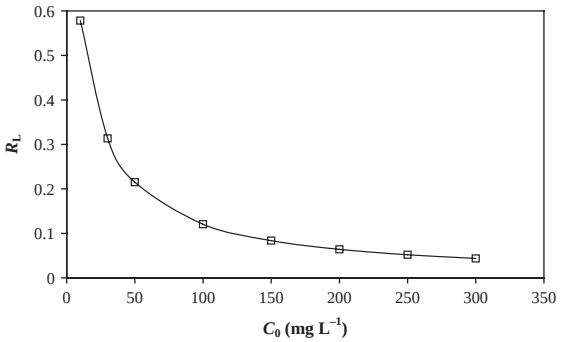

Fig. 8. Separation factors for MG onto eucalyptus bark for different initial dye concentrations at 20 °C.

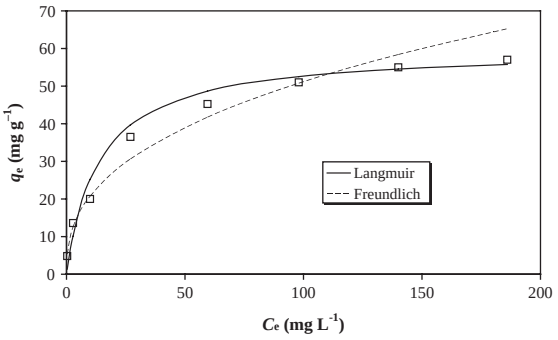

Fig. 9. Comparison of experimental and predicted sorption isotherms of MG onto eucalyptus bark according to Langmuir and Freundlich equations at 20 °C.

all initial dye concentrations confirms the favorable uptake of MG process.

3.4.2. Freundlich model

The Freundlich equation can be written as

$$q_e = K_F C_e^{1/n} \quad (5)$$

where q_e is the amount of solute sorbed per unit weight of sorbent (mg g^{-1}), C_e is the equilibrium concentration of solute in the bulk solution (mg L^{-1}), K_F is a constant indicative of the relative sorption capacity of the sorbent (mg$^{1-\frac{1}{n}}$ L$^{\frac{1}{n}}$ g^{-1}), and n is a constant indicative of the intensity of the sorption. The Freundlich expression is an exponential equation and therefore, assumes that as the sorbate concentration increases, the concentration of sorbate on the sorbent surface also increases. The linear form of the Freundlich isotherm is

$$\ln q_e = \ln K_F + \frac{1}{n} \ln C_e \quad (6)$$

The equilibrium data were further analyzed using the linearized form of Freundlich equation using the same set experimental data, by plotting ln q_e versus ln C_e (figure not shown). The calculated Freundlich isotherm constants and the corresponding coefficient of determination values were shown in Table 1. From Table 1, it was observed that both the Freundlich and Langmuir isotherms could well represent the experimental sorption data of MG by eucalyptus bark, but the Langmuir expression was better.

The magnitude of the exponent n gives an indication on the favorability of sorption. It is generally stated that values of n in the range 2–10 represent good, 1–2 moderately difficult, and less than 1 poor adsorption characteristics [19]. The value of the Freundlich parameter n shows that the studied material is good sorbent for MG.

The applicability of both Langmuir and Freundlich isotherms to the studied system implies that both monolayer sorption and heterogeneous surface conditions exist under the used experimental conditions.

Fig. 9 shows the experimental equilibrium data as well as the theoretical curves predicted by the Langmuir and Freundlich models. It was observed that the equilibrium data were well represented by the Langmuir isotherm equation when compared to the Freundlich model.

3.5. Modeling of sorption kinetics

In order to investigate the kinetics of MG sorption by eucalyptus bark, the Lagergren pseudo-first-order model [20] and the Ho's linear form [21,22] of the pseudo-second-order model, developed by Blanchard et al. [23], were used.

A simple kinetic analysis of sorption can be performed with a pseudo–first–order equation as suggested by Lagergren [20]

$$\frac{dq}{dt} = K_1 (q_e - q) \quad (7)$$

where K_1 (min^{-1}) is the rate constant of the pseudo-first-order sorption, q_e (mg g^{-1}) is the amount of dye sorbed on the sorbent surface at equilibrium, and q (mg g^{-1}) is the amount of dye sorbed at any time t (min).

Eq. (7) above can be integrated to the following form by applying the boundary conditions $q = 0$ at $t = 0$

$$\ln(q_e - q) = \ln q_e - K_1 t \quad (8)$$

This rate expression is known as the Lagergren pseudo-first-order equation.

Since $q = 0$ at $t = 0$, the initial rate of adsorption can be calculated from Eq. (9) as follows:

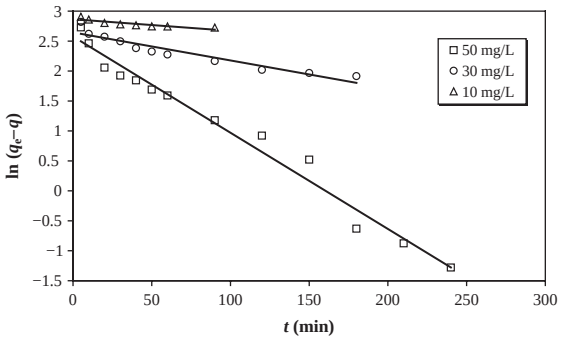

Fig. 10. Pseudo-first-order kinetics for sorption of MG onto eucalyptus bark at 20 °C.

$$h_1 = K_1 q_e \tag{9}$$

The values of K_1 and q_e can be determined by the slope of linear plots of ln $(q_e - q)$ versus t (Fig. 10). The parameters of the pseudo-first-order model are summarized in Table 2. The values of determination coefficient for the plots were in the range 0.770–0.978. However, although the coefficient of determination value is reasonably high for an initial dye concentration of 50 mg L^{-1}, the calculated sorption capacity values obtained from this kinetic model do not give reasonable values compared with experimental sorption capacity. This finding suggested that the sorption process does not follow the pseudo-first-order sorption rate expression of Lagergren.

An expression of the pseudo–second–order rate based on the solid capacity has been presented by Blanchard [23]

$$\frac{dq}{dt} = K_2 (q_e - q)^2 \tag{10}$$

where K_2 is the pseudo-second-order rate constant (g mg^{-1} min^{-1}), q_e is the amount of dye sorbed at equilibrium (mg g^{-1}), and q is the amount of dye cation on the surface of the sorbent at any time t (mg g^{-1}).

Integrating Eq. (10), considering that $q = 0$ when $t = 0$ and that $q = q$ when $t = t$, results in the expression [21,22]

$$\frac{t}{q} = \frac{1}{K_2 q_e^2} + \frac{1}{q_e} t \tag{11}$$

The initial sorption rate h (mg g^{-1} min^{-1}) is given by the following equation

$$h_2 = K_2 q_e^2 \tag{12}$$

By plotting t/q versus t (Fig. 11), q_e and K_2 can be determined from slope and intercept. As mentioned above, the curve fitting plots of ln $(q_e - q)$ versus t does not show good results, while the plots of t/q versus t give a straight line for all the initial dye concentrations studied as showed in Fig. 11, confirming the applicability of the pseudo-second-order equation. The parameters of the pseudo-second-order sorption kinetic model are tabulated in Table 2. The determination coefficient values of the pseudo-second-order model exceeded 0.99 and the calculated sorption capacity values determined from pseudo-second-order model were more consistent with the experimental values of sorption capacity. Therefore, the pseudo-second-order model better represented the sorption kinetics and thus supports the assumption behind the model. This suggests that the overall rate of the MG sorption process appeared to be controlled by chemical process.

3.5.1. Sorption mechanism

From design aspect, it is important to estimate which is the rate-limiting step (pore or film diffusion) involved in the sorption process. The three consecutive steps in the sorption of a sorbate by a sorbent are:

- Transport of sorbate molecules from the bulk solution to the external surface of the sorbent by diffusion across the liquid boundary layer (film diffusion).

Table 2
Parameters of the pseudo-first-order and the pseudo-second-order models for the sorption of MG by eucalyptus bark for different initial dye concentrations (sorbent dosage = 0.4 g/200 mL, T = 20 °C, pH 5)

C_0 (mg L^{-1})	$q_{e\,exp}$ (mg g^{-1})	Pseudo-first-order model				Pseudo-second-order model			
		K_1 (min^{-1})	$q_{e\,calc}$ (mg g^{-1})	h_1 (mg g^{-1} min^{-1})	R^2	K_2 (g mg^{-1} min^{-1})	$q_{e\,calc}$ (mg g^{-1})	h_2 (mg g^{-1} min^{-1})	R^2
10	4.84	1.95×10^{-3}	17.56	0.034	0.770	28.24×10^{-3}	4.98	0.701	0.999
30	13.60	4.68×10^{-3}	14.08	0.066	0.903	3.23×10^{-3}	14.58	0.686	0.999
50	20.02	16.10×10^{-3}	13.14	0.212	0.978	2.30×10^{-3}	21.37	1.048	0.999

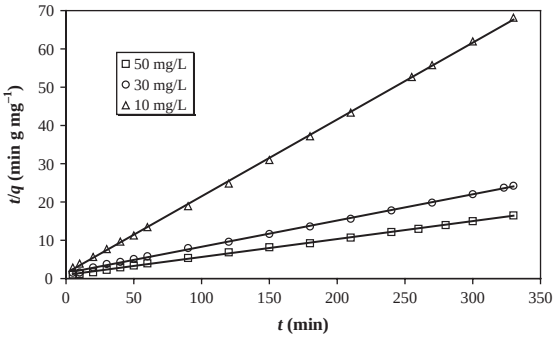

Fig. 11. Pseudo-second-order kinetics for sorption of MG onto eucalyptus bark at 20 °C.

- Diffusion of the sorbate within the pores of the sorbent (intraparticle diffusion).
- Sorption of the sorbate on the active sites.

It is generally accepted that the last step is usually very rapid in comparison to the first two steps. Therefore, the overall rate of sorption is controlled by either film or intraparticle diffusion.

Since neither the pseudo-first-order nor the pseudo-second-order model can identify the diffusion mechanism, the kinetic results were analyzed by the intraparticle diffusion model.

The rate parameter of intraparticle diffusion can be defined as [24]

$$q = k_{id}\, t^{1/2} + c \tag{13}$$

where q (mg g^{-1}) is the amount of MG sorbed at time t, c (mg g^{-1}) the intercept, and k_{id} (mg g^{-1} $min^{-1/2}$) is the intraparticle diffusion rate constant.

The kinetic results can be used to determine if particle diffusion is the rate-limiting step for dye sorption onto material. Fig. 12 shows the amount of dye sorbed versus $t^{1/2}$ for intraparticle transport of MG by

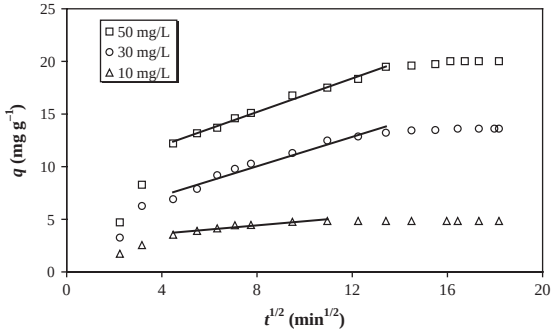

Fig. 12. Plots for evaluating intraparticle diffusion rate constant for sorption of MG onto eucalyptus bark (sorbent dosage = 0.4 g/200 mL, T = 20 °C, pH 5).

Table 3
Intraparticle diffusion parameters for the sorption of MG at various initial dye concentrations (sorbent dosage = 0.4 g/200 mL, T = 20 °C, pH 5)

C_0 (mg L^{-1})	k_{id} (mg g^{-1} $min^{-1/2}$)	c (mg g^{-1})	R^2
10	0.197	2.84	0.910
30	0.698	4.45	0.960
50	0.798	8.81	0.994

eucalyptus bark at different initial dye concentrations. It can be observed that the plots had the same general features and there were three different portions, representing the different stages in sorption: an initial curve portion followed by linear portion and a plateau. The initial curve portion was due to surface sorption and rapid external diffusion (boundary layer diffusion). The second linear portion is the gradual sorption stage where the intraparticle diffusion is rate-controlled. The plateau (third portion) is the final equilibrium stage, where the intraparticle diffusion starts to slow down due to the low solute concentration in solution.

The slope of the second linear portion characterizes the rate parameter corresponding to the intraparticle diffusion, whereas the intercept of this portion is proportional to the boundary layer thickness. The calculated k_{id} values for each initial concentration are given in Table 3. It was found that the rate constant increased with increasing dye concentration. The determination coefficient values for this diffusion model are between 0.910 and 0.994 (Table 3). This indicates that the sorption of MG onto sorbent material can be followed by an intraparticle diffusion model after 20 min. The double initial nature of the curve reflects the two-stage external diffusion (mass transfer) followed by intraparticle diffusion of dye onto sorbent. However, the results do not pass through the origin (the plots have intercepts in the range 2.84–8.81 mg g^{-1}), indicating that intraparticle diffusion is involved in the sorption process but it is not the only rate–limiting mechanism and that some other mechanisms also play an important role. The values of the intercept also give an idea about the boundary layer thickness: the larger the intercept, the greater is the boundary layer effect. Namely, any increase in the value of c indicates the abundance of solute in the boundary layer. As seen in Table 3, the value of c increases with increasing concentration.

3.6. Eucalyptus bark performance

Table 4 compares the sorption capacity of different types of sorbents used for removal of MG. The value

Table 4
Reported maximum sorption capacities in the literature for MG

Sorbent	q_m (mg g^{-1})	References
Bagasse fly ash	170.33	[5]
Treated rice husks	92.5	[25]
Cyclodextrin-based adsorbent	91.9	[2]
Activated slag	74.16	[26]
Treated sawdust	65.8	[27]
Eucalyptus bark	59.88	This work
Laboratory grade activated carbons	42.18	[5]
Activated carbons commercial grade	8.27	[5]
Bentonite clay	7.72	[29]
Sugar cane dust	4.88	[28]
Activated charcoal	0.179	[30]

of monolayer sorption capacity in this study is comparable to the sorption capacities of some other sorbent materials for MG. This suggests that MG could be easily sorbed by eucalyptus bark.

4. Conclusions

Kinetic and equilibrium studies were reported for the sorption of MG from aqueous solutions by eucalyptus bark. Results of sorption showed that eucalyptus bark, an abundant forest waste, can be effectively used as a sorbent for the removal of dye.

Experimental data indicated that the amount of dye sorbed was dependent of operating variables such as contact time, initial dye concentration, sorbent dosage, and temperature. Modeling of sorption kinetics showed good agreement of experimental data with the pseudo-second-order kinetic equation for different initial dye concentrations.

The equilibrium sorption data were analyzed by the Langmuir and the Freundlich isotherm equations. The Langmuir model yielded a much better fit than the Freundlich model. The monolayer sorption capacity of eucalyptus bark based on Langmuir model was found to be 59.88 mg g^{-1} at 20 °C.

The overall rate of dye uptake was found to be controlled by external mass transfer at the beginning of sorption, while intraparticle diffusion controlled the overall rate of sorption at a later stage.

Acknowledgements

The financial support from the Ministry of Higher Education and Scientific Research of Algeria (Project No. J0101120060043) is gratefully acknowledged.

Nomenclature

b	Langmuir constant (L mg^{-1})
c	intercept of the intraparticle diffusion model (mg g^{-1})
C_0	the initial concentration of the solute in the bulk solution (mg L^{-1})
C_e	the equilibrium concentration of the solute in the bulk solution (mg L^{-1})
h_1	initial sorption rate for the pseudo-first-order model (mg g^{-1} min^{-1})
h_2	initial sorption rate for the pseudo-second-order model (mg g^{-1} min^{-1})
k_{id}	the intraparticle diffusion rate constant (mg g^{-1} $min^{-1/2}$)
K_1	Lagergren pseudo-first-order rate constant (min^{-1})
K_2	the pseudo-second-order rate constant (g mg^{-1} min^{-1})
K_F	Freundlich constant indicative of the relative sorption capacity of the sorbent ($mg^{1-\frac{1}{n}}$ $L^{\frac{1}{n}}$ g^{-1})
n	Freundlich constant indicative of the intensity of the sorption
q	the amount of solute sorbed at any time t (mg g^{-1})
q_e	the amount of solute sorbed per unit weight of sorbent at equilibrium (mg g^{-1})
q_m	the maximum sorption capacity (mg g^{-1})
R^2	coefficient of determination
R_L	dimensionless separation factor of Hall
t	Time (min)

References

[1] I.M. Banat, P. Nigam, D. Singh and R. Marchant, Microbial decolourization of textile-dye containing effluents: a review, Bioresour. Technol., 58 (1996) 217-227.
[2] G. Crini, H.N. Peindy, F. Gimbert and C. Robert, Removal of C.I. Basic Green 4 (Malachite Green) from aqueous solutions by adsorption using cyclodextrin-based adsorbent: kinetic and equilibrium studies, Sep. Purif. Technol., 53 (2007) 97-110.
[3] A. Mittal, L. Krishnan and V.K. Gupta, Removal and recovery of malachite green from wastewater using an agricultural waste material, de-oiled soya, Sep. Purif. Technol., 43 (2005) 125-133.
[4] V.K. Garg, R. Kumar and R. Gupta, Removal of malachite green dye from aqueous solution by adsorption using agro-industry waste: a case study of *Prosopis cineraria*, Dyes Pigments, 62 (2004) 1-10.
[5] I.D. Mall, V.C. Srivastava, N.K. Agarwal and I.M. Mishra, Adsorptive removal of malachite green dye from aqueous solution by bagasse fly ash and activated carbon-kinetic study and equilibrium isotherm analyses, Colloids Surf A Physicochem. Eng. Aspects, 264 (2005) 17-28.
[6] A. Mittal, Adsorption kinetics of removal of a toxic dye, Malachite Green, from wastewater by using hen feathers, J. Hazard. Mater., B133 (2006) 196-202.
[7] P. Janoš, V. Šmídová, Effects of surfactants on the adsorptive removal of basic dyes from water using an organomineral sorbent—iron humate, J. Colloid Interface Sci., 291 (2005) 19-27.

[8] R. Gong, Y. Jin, F. Chen, J. Chen and Z. Liu, Enhanced malachite green removal from aqueous solution by citric acid modified rice straw, J. Hazard. Mater., 137 (2006) 865-870.
[9] K.V. Kumar and K. Porkodi, Batch adsorber design for different solution volume/adsorbent mass ratios using the experimental equilibrium data with fixed solution volume/adsorbent mass ratio of malachite green onto orange peel, Dyes Pigments, 74 (2007) 590-594.
[10] T.G. Chuah, A. Jumasiah, I. Azni, S. Katayon and S.Y. Thomas Choong, Rice husk as a potentially low-cost biosorbent for heavy metal and dye removal: an overview, Desalination, 175 (2005) 305-316.
[11] L.C. Morais, O.M. Freitas, E.P. Gonçalves, L.T. Vasconcelos and C.G. González Beça, Reactive dyes removal from wastewaters by adsorption on eucalyptus bark: variables that define the process, Water Res., 33 (1999) 979-988.
[12] L.C. Morais, E.P. Gonçalves, L.T. Vasconcelos and C.G. González Beça, Reactive dyes removal from wastewaters by adsorption on eucalyptus bark – adsorption equilibria, Environ. Technol., 21 (2000) 577-583.
[13] R. Saliba, H. Gauthier, R. Gauthier and M. Petit-Ramel, The use of eucalyptus barks for the adsorption of heavy metal ions and dyes, Adsorp. Sci. Technol., 20 (2002) 119-129.
[14] V.K. Garg, M. Amita, R. Kumar and R. Gupta, Basic dye (methylene blue) removal from simulated wastewater by adsorption using Indian Rosewood sawdust: timber industry waste, Dyes Pigments, 63 (2004) 243-250.
[15] D.D. Das, R. Mahapatra, J. Pradhan, S.N. Das and R.S. Thakur, Removal of Cr (VI) from aqueous solution using activated cow dung carbon, J. Colloid Interface Sci., 232 (2000) 235-240.
[16] Y. Guo, J. Qi, S. Yang, K. Yu, Z. Wang and H. Xu, Adsorption of Cr(VI) on micro and mesoporous rice husk-based active carbon, Mater. Chem. Phys., 78 (2002) 132-137.
[17] I. Ghodbane, O. Hamdaoui, Removal of mercury(II) from aqueous media using eucalyptus bark: Kinetic and equilibrium studies, J. Hazard. Mater., 160 (2008) 301-309.
[18] K.R. Hall, L.C. Eagleton, A. Acrivos and T. Vermeulen, Pore and solid diffusion kinetics in fixed–bed adsorption under constant pattern conditions, Ind. Eng. Chem. Fundam., 5 (1966) 212-223.
[19] R.E. Treybal, Mass-Transfer Operations, 3rd ed., McGraw Hill, 1981.
[20] S. Lagergren, About the theory of so-called adsorption of soluble substances, Kungliga Svenska Vetenskapsakademiens, Handlingar, 24(4) (1898) 1-39.
[21] Y.S. Ho, Adsorption of Heavy Metals from Waste Streams by Peat, PhD Thesis, University of Birmingham, Birmingham, UK, 1995.
[22] Y.S. Ho and G. McKay, The kinetics of sorption of divalent metal ions onto sphagnum moss peat, Water Res., 34 (2000) 735-742.
[23] G. Blanchard, M. Maunaye and G. Martin, Removal of heavy metals from waters by means of natural zeolites, Water Res., 18 (1984) 1501-1507.
[24] W.J. Weber Jr., J.C. Morris, Kinetics of adsorption on carbon from solution, J. Sanitary Eng. Div., 89 (1963) 31-59.
[25] I.A. Rahman, B. Saad, S. Shaidan and E.S. Sya Rizal, Adsorption characteristics of malachite green on activated carbon derived from rice husks produced by chemical–thermal process, Bioresour. Technol., 96 (2005) 1578-1583.
[26] V.K. Gupta, S.K. Srivastava and D. Mohan, Equilibrium uptake, sorption dynamics, process optimization, and column operations for the removal and recovery of malachite green from wastewater using activated carbon and activated slag, Ind. Eng. Chem. Res., 36 (1997) 2207-2218.
[27] K.V. Kumar, S. Sivanesan and V. Ramamurthi, Adsorption of malachite green onto *Pithophora* sp., a fresh water algae: equilibrium and kinetic modelling, Process. Biochem., 40 (2005) 2865-2872.
[28] S.D. Khattri and M.K. Singh, Colour removal from dye wastewater using sugar cane dust as an adsorbent, Adsorp. Sci. Technol., 17 (1999) 269-282.
[29] S.S. Tahir and N. Rauf, Removal of a cationic dye from aqueous solutions by adsorption onto bentonite clay, Chemosphere, 63 (2006) 1842-1848.
[30] M.J. Iqbal and M.N. Ashiq, Adsorption of dyes from aqueous solutions on activated charcoal, J. Hazard. Mater., B139 (2007) 57-66.